Letter to the Editor

HCN in the inner envelope of χ Cygni

D. Duari[1,2] **and J. Hatchell**[1]

[1] Department of Physics, UMIST, P O Box 88, Manchester M60 1QD, UK
[2] The Birla Institute of Astronomy and Planetary Sciences, Calcutta 700 071, India

Abstract. We have detected the $(0, 1^{1c}, 0)\, J = 3\text{–}2$ and $(0, 0, 0)\, J = 8\text{–}7$ transitions of HCN towards the S star χ Cygni. The excitation requirements of these transitions are too high to be satisfied in the outer envelope of the star, and the emission must originate within $\gtrsim 20$ stellar radii, ie. the molecule must be forming close to the star. This conclusion is supported by a model for AGB stars in which molecules including HCN form in a shocked wind close to the stellar surface.

Key words: stars: AGB and post-AGB – stars: circumstellar matter – stars: individual: χ Cyg – submillimeter

1. Introduction

Recent detections of warm carbon bearing molecules in different O-rich AGB stars suggest that these carbon species have to form in the deep layers of the stellar wind. Photochemical models (Willacy & Millar 1997) of several O-rich stars, which rely on injection of certain molecules to generate a carbon-rich chemistry at large radii, succeed in reproducing the observed values of certain molecules but fail to reproduce some molecular abundances, in particular that of HCN. HCN is observed in the envelope of several O- and S-type stars at abundances of $> 10^{-6}$ (Bieging & Latter 1994 (BL94); Bujarrabal et al. 1994; Sopka et al. 1989).

Duari et al. (1999) (DCW99) considered whether a shocked wind model could reproduce HCN abundances for O-rich objects. Local thermodynamic equilibrium (LTE) models fail to reproduce the observed abundances by several orders of magnitude (BL94). An investigation of non-equilibrium chemistry of the oxygen rich Mira IK Tau showed that these carbon bearing molecules can efficiently form in the inner regions close to the stellar photosphere (DCW99). In this case, it was shown that applications of stellar pulsation induced shocks in a narrow region of the photosphere can give rise to molecular processes in the immediate cooling layer and the hydrodynamic cooling part (= excursion) of the post shock region and can produce certain carbon bearing molecules including HCN and CO_2.

Table 1. Observing parameters: transitions and frequencies; receivers; beam diameter (full width half maximum); zenith opacity at 225 GHz; main beam efficiency and system temperature; RMS noise levels on 1 km s^{-1} channels.

line	HCN 3–2 $(0,0,0)$ & $(0,1^{1c},0)$	H^{13}CN 3–2 $(0,0,0)$	HCN 8–7 $(0,0,0)$
ν/GHz	265.8862 & 265.8527	259.0118	708.8772
receiver	A3	A3	W
FWHM	18$''$	18$''$	8$''$
τ_{225}	0.04	0.1	0.04
η_{MB}	0.69	0.69	0.30
T_{sys}	270	400	3500–5000
T_{MB} (rms)	0.014	0.030	0.28

It was earlier noted for S-type stars (Bujarrabal et al. 1994) that their molecular line strengths are almost equidistant between those of C- and O- rich objects. This property has been argued to be related to the fact that the atmospheric C/O ratio is close to the value of 1 and intermediate to that of O- and C- rich evolved stars. We therefore apply DCW99's chemical model, which successfully reproduces the observed HCN abundances in O-rich objects, to the intermediate case of S stars. In tandem we have looked for observational evidence that the HCN is forming in the inner envelope the S star χ Cyg. Although HCN has previously been detected in χ Cyg, the lines observed are dominated by material at large radii, so here we look for high excitation transitions. In carbon stars, such transitions are detected in the inner regions of the winds (eg. Lucas & Guilloteau 1992).

In Sect. 2 we describe the observations and in Sect. 3 demonstrate that the HCN detected must lie in the inner parts of the circumstellar envelope, a result which is strongly supported by our modelling of the inner wind region of χ Cyg (Sect. 4). Our conclusions are in Sect. 5.

2. Observations and results

Observations were made during 1999 using the James Clerk Maxwell Telescope (JCMT) on Mauna Kea, Hawaii. We observed the vibrationally excited HCN $(0, 1^{1c}, 0)\, J = 3\text{–}2$ line at 266 GHz, the $(0, 1^{1d}, 0)$ and $(0, 2^0, 1)\, J = 3\text{–}2$

Table 2. Integrated intensities and upper state column densities for detected transitions.

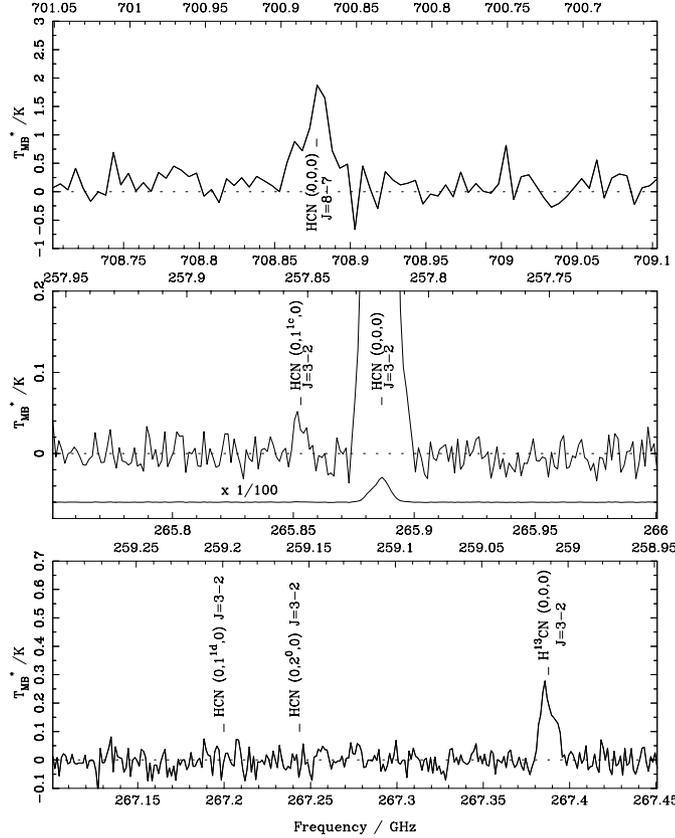| transition	HCN 3–2 $v_2 = 0$	H^{13}CN 3–2 $v_2 = 0$	HCN 3–2 $v_2 = 1$	HCN 8–7
frequency/GHz	265.8862	259.0118	265.8527	708.8772
$\int T_{\mathrm{MB}} \, \mathrm{d}v/\mathrm{K\,km\,s^{-1}}$	20.31	1.38	0.15	0.30
$N_{\mathrm{U}}/\mathrm{cm}^{-2}$	4.8×10^{12}	3.4×10^{11}	3.6×10^{10}	1.1×10^{12}

Fig. 1. HCN spectra towards χ Cyg: (top) HCN 8–7; (centre) HCN $(0,0,0)$ and $(0,1^{1c},0)$ $J-3$–2 (also offset and scaled by $1/100$); (bottom) H^{13}CN 3–2 with the positions of the $(0,1^{1d},0)$ and $(0,2^0,0)$ non-detections indicated.

lines at 267 GHz, and HCN $(0,0,0)$ $J = 8$–7 at 709 GHz. The pointing centre was the Hipparcos position of χ Cyg, $19^{\mathrm{h}} 50^{\mathrm{m}} 33.^{\mathrm{s}}92 +32° 54' 50.''6$ (Perryman et al. 1997). Observing parameters are given in Table 1.

We detected HCN $J = 8$–7 and the $(0,1^{1c},0)$ $J = 3$–2 line at 266 GHz. The spectra are shown in Fig. 1. The HCN $(0,1^{1d},0)$ and $(0,2^0,0)$ lines at 267 GHz were not detected: though this $v_2 = 1$ line should be the same strength as the one detected at 266 GHz, this spectrum had a higher noise level (the frequencies are marked in Fig. 1). The HCN and H^{13}CN $J = 3$–2 ground state lines at 266 and 259 GHz were also detected.

3. Excitation analysis

The excitation requirements of the $J = 8$–7 and $(0,1^{1c},0)$ $J = 3$–2 transitions are high. We consider whether collisional or

radiative excitation mechanisms can produce the observed line intensities.

The column densities in each state can be determined from the observed integrated line intensities, assuming they are optically thin. For HCN this conversion is:

$$\left(\frac{N_{\mathrm{U}}}{\mathrm{cm}^{-2}}\right) = 1.876 \times 10^{13} \left(\frac{\nu}{\mathrm{GHz}}\right)^{-1} \frac{(2J+1)}{(J+1)}$$
$$\times \left(\frac{\int T_{\mathrm{MB}} \, \mathrm{d}v}{\mathrm{K\,kms^{-1}}}\right) \tag{1}$$

where J is the rotational quantum number of the transition $J + 1 \rightarrow J$, and we assume excitation temperatures much higher than the 2.7 K background. The resulting column densities are given in Table 2.

We use the H^{13}CN $(0,0,0)$ $J = 3$–2 as a surrogate for the equivalent H^{12}CN line as it is more likely to be optically thin. We assume the same excitation in H^{13}CN as H^{12}CN, and a $[^{12}\mathrm{C}]/[^{13}\mathrm{C}]$ ratio, which is unknown in χ Cyg. Sopka et al. (1989) found $[^{12}\mathrm{C}]/[^{13}\mathrm{C}] > 5$ from H^{12}CN/H^{13}CN 1–0 observations. From the ratio of our H^{12}CN and H^{13}CN transitions, $[^{12}\mathrm{C}]/[^{13}\mathrm{C}] \gtrsim 12$. (This ratio also supports our assumption that the H^{13}CN is optically thin.) However, these low limits do not rule out a much higher value. We take as an upper limit a typical ISM value of 70.

Assuming purely collisional excitation,

$$\frac{N_{\mathrm{L}}}{N_{\mathrm{U}}} = \frac{g_{\mathrm{L}}}{g_{\mathrm{U}}} (n_{\mathrm{crit}}/n_{\mathrm{H_2}} + 1) e^{h\nu/kT_{\mathrm{kin}}}, \tag{2}$$

where N_{U}, N_{L}, g_{U} and g_{L} are the upper and lower state column densities and degeneracies and $n_{\mathrm{H_2}}$ the unknown hydrogen column density. The critical densities for both transitions are high: for the $(0,1^{1c},0)$ $J = 3$ state we calculate $n_{\mathrm{crit}} \simeq 4.8 \times 10^{11} \mathrm{cm}^{-3}$ (following Stutzki et al. 1988), and for $J = 8$–7 $n_{\mathrm{crit}} \simeq 1.2 \times 10^9 \mathrm{cm}^{-3}$. Applying Eq. 2 together with the column densities from Table 2, the minimum density requirements to achieve the observed ratios are 1×10^9 and $5 \times 10^7 \mathrm{cm}^{-3}$ for $(0,1^{1c},0)$ $J = 3$–2 and $J = 8$–7 transitions respectively. For $J = 8$–7 we assume the population in $J = 7$ is the same or less than that measured in $J = 3$.

The envelope gas density falls off very rapidly with radius (Bertschinger & Chevalier 1985; Cherchneff et al. 1992). Assuming the stellar parameters for χ Cyg given in Table 3, the total hydrogen density at $1R_\star$ is $3.6 \times 10^{15} \mathrm{cm}^{-3}$ and the density falls below the density requirement for $(0,1^{1c},0)$ $J = 3$–2 within $3.5R_\star$ and for $J = 8$–7 within $5R_\star$. Alternatively, assuming a density profile due to steady mass loss of $1.8 \times 10^{-7} \mathrm{M_\odot yr^{-1}}$ at $8.9 \mathrm{km\,s^{-1}}$ (BL94), then the density at $1R_\star$ is $7.5 \times 10^8 \mathrm{cm}^{-3}$ and falls as R^{-2}. This constrains the HCN 8–7 emission to within $\sim 4R_\star$, assuming it is collisionally excited.

An alternative means of exciting these HCN transitions is by radiative pumping by the IR radiation from the star. The $(0, 0, 0)$ and $(0, 1, 0)$ states are connected by $14\,\mu$m radiation with an Einstein A coefficient of 3.7s^{-1} (Ziurys 1986). If collisions can be neglected, and assuming geometrical dilution of the stellar radiation field, the ratio of column densities in the ground and $v_2 = 1$ vibrational states depends on the distance from the star according to the formula:

$$\frac{N_{\text{L}}}{N_{\text{U}}} = (e^{h\nu/kT_\star} - 1)(2R/R_\star)^2 + 1 \qquad (3)$$

with R radius and $T_\star$ stellar temperature. Assuming a stellar temperature of 2200 K, this constrains the radius at which the $(0, 1^{1c}, 0)$ line is emitted to $R \gtrsim 17R_\star$.

The $(0, 0, 0)$ $J = 8$ state cannot be directly pumped by radiation (as $\Delta J = 0, \pm 1$ for HCN) but it could be populated through successive excitations to the $(0, 1, 0)$ levels in increasing J states. The radius requirements for this to take place are stronger than for the $(0, 1^{1c}, 0)$ state.

For either collisional or radiative excitation, the radius requirements are tightened further if either (a) $[^{12}\text{C}]/[^{13}\text{C}] < 70$ or (b) H^{13}CN $J = 3$–2 emission originates from a larger region than HCN $(0, 1^{1c}, 0)$ $J = 3$–2 or HCN $J = 8$–7.

To conclude, the excitation requirements are such that both the HCN $(0, 1^{1c}, 0)$ $J = 3$–2 and HCN $J = 8$–7 transitions must originate from gas within $\gtrsim 20$ stellar radii, in the inner envelope of the star, whether collisionally or radiatively excited.

4. Model of the inner wind of χ Cyg

We have used our chemical model, which has succesfully produced the observed HCN abundance in the case of an O-rich object (see DCW99 for details), with a value of C/0 $\sim$ 1 for modelling the inner wind region of χ Cyg. The stellar parameters considered in this study are listed in Table 3. The radius is obtained from the observational value of Tuthill et al. (1999) and the pulsation period is from Bedding & Zijlstra (1998). Using the standard pulsation equation for Miras of Fox and Wood (1982) and assuming that the star is pulsating in its fundamental mode ($Q = 0.09$), we derive a stellar mass of 1.15 M$_\odot$, which is a typical value for the stars of this class. The temperature of 2200 K was obtained from Haniff et al. (1995) which gave a luminosity which is close to the canonical value for typical Miras.

We have considered here the inner wind above the photospheric region which experiences passage of strong, periodic shocks generated by stellar pulsation. The model deals with the chemistry of the immediate region (thermal cooling region) and the hydrodynamical cooling region of post shock described by Bertschinger & Chevalier (1985), Fox & Wood (1985) and Willacy & Cherchneff (1998).

4.1. The chemistry

We have considered 760 reactions involving 68 chemical species and have all possible chemical routes possible in a dense gas. The reaction rates considered are the same as in DCW99 (and

Table 3. χ Cyg - stellar parameters: γ and α are defined as in Cherchneff et al. (1992) and X (Y) $\equiv$ X $\times$ 10^{Y}.

D	106 pc	$\dot{M}$	$1.8(-7)\text{M}_\odot\text{yr}^{-1}$
$T_\star$	2200 K	$L_\star$	$1.8(3)$ L$_\odot$
$R_\star$	290 R$_\odot$	$M_\star$	1.15 M$_\odot$
P	408 days	$n(r_{\text{shock}})$	$3.6\,(15)\,\text{cm}^{-3}$
r_{shock}	$1.0\,\text{R}_\star$	α	0.6
$\gamma = v_{\text{shock}}/v_{\text{esc}}$	0.89	C/O ratio	0.95

the references therein). We have assumed thermal equilibrium for the photosphere and derived molecular abundances for the temperature, C/O ratio and gas density given in Table 3. We then apply a shock to the photosphere (the shock velocity considered is $v_{shock} = 32$ Km s^{-1}) and study the chemistry in the immediate and excursion region. The resulting abundances form the input for the shock at the next distance. The different parameters describing the shock structure at different radial distances from the star is given in Table 4.

4.2. Model results and discussion

The molecular abundances of few selected species relative to the total gas number density are given in Table 5 for various shock strengths. We have considered shock chemistry at gas layers very close to the star. The abundances at $2R_\star$ may not be the exact values in the outflow because of uncertainties in the dust formation radius which halts the shock chemistry, but are indicative. One can see that in addition to molecular hydrogen certain other molecules like CO, H$_2$O and N$_2$ are dominant, confirming that they are the parent molecules. But, to come to the point of our interest, the shock chemistry is responsible for formation of species like HCN along with CO$_2$ and CS close to the star. The prediction of HCN at the distance and environment described is in excellent agreement with the observational result of Sect. 2. Moreover, the theoretical value obtained for the HCN abundance is in agreement with that derived from millimeter line observations in the outer wind.

The chemical processes responsible for the formation of HCN involves reactions with cyanogen - an observation which was earlier found to be the case in O-rich IK Tau (DCW99). HCN is formed by the reaction

$$\text{CN} + \text{H}_2 \rightarrow \text{HCN} + \text{H} \qquad (4)$$

CN acts as an intermediary in the formation of HCN and CS and is destroyed quickly by atomic hydrogen. The reaction is sensitive to temperature and is very fast in the gas excursions. On the basis of the chemistry we can claim that HCN is a direct result of the shock chemistry in the inner wind region that we have considered here and travels as a parent species through the envelope unaltered until it reaches the photo-dissociation regions in the outer wind. The choice of the ratio C/O=0.95 is arbitrary, but with different values of C/O equal or slightly greater than 1.0, though the T.E. abundance values differ by a factor of 100, yet the resulting HCN abundance at $2R_*$ remains within 5 percent of the quoted number in Table 5.

Table 4. Pre-shock, shock front and excursion ($\equiv$ post-shock) gas temperature and number density as a function of position in the envelope and shock strengths. M is the Mach number associated with each shock speed.

Position ($R_\star$)	Shock Vel. (km s^{-1})	M	Pre-shock		Shock Front		Start of excursion	
			T_0 (K)	n_0 (cm^{-3})	T (K)	n (cm^{-3})	T (K)	n (cm^{-3})
1.0	32.0	10.3	2200	3.62 (15)	47458	2.07 (16)	6528	1.26 (17)
1.5	26.1	9.51	1724	1.28 (13)	31959	7.28 (13)	4867	3.98 (14)
2.0	22.6	8.98	1452	3.93 (11)	24128	2.22 (12)	3966	1.13 (13)

Table 5. Calculated fractional abundances (relative to the total gas number density) versus shock strength and radius.

Species	T.E. 1. R$_\star$	32 km s^{-1} 1. R$_\star$	26.1 km s^{-1} 1.5 R$_\star$	22.6 km s^{-1} 2. R$_\star$
H	1.0(-01)	4.3(-03)	4.4(-03)	4.2(-01)
H$_2$	7.3(-01)	8.2(-01)	8.1(-01)	4.4(-01)
S	1.5(-05)	2.0(-06)	2.9(-06)	1.6(-05)
C$_2$H$_2$	1.5(-15)	3.6(-11)	4.6(-12)	4.9(-15)
CS	3.4(-09)	1.5(-05)	2.0(-05)	3.0(-06)
HS	4.8(-06)	4.3(-06)	1.1(-06)	7.0(-09)
H$_2$S	4.8(-07)	4.8(-07)	4.8(-08)	7.2(-13)
NS	4.6(-11)	7.3(-12)	2.9(-11)	9.4(-13)
N	3.4(-09)	3.0(-13)	7.6(-17)	1.1(-17)
N$_2$	9.0(-05)	5.8(-06)	5.3(-05)	7.1(-05)
HCN[†]	**1.6(-09)**	**1.8(-04)**	**8.5(-05)**	**4.8(-06)**
CN	1.4(-11)	4.6(-09)	6.2(-10)	1.9(-09)
O	2.6(-08)	8.4(-11)	1.1(-11)	8.7(-10)
OH	2.0(-07)	3.0(-08)	3.7(-09)	1.1(-08)
H$_2$O	7.4(-06)	2.0(-04)	1.1(-04)	5.6(-06)
CO	9.9(-04)	8.5(-04)	8.6(-03)	6.6(-03)
CO$_2$	2.0(-09)	6.4(-08)	8.3(-07)	4.7(-06)
O$_2$	1.2(-13)	6.8(-15)	5.5(-16)	5.3(-15)
SiO	4.4(-05)	4.7(-05)	5.0(-05)	3.9(-05)

[†] The observation value for HCN (averaged over the entire envelope) is **2.5(-6)** derived from millimeter observations (Bujarrabal et al. 1994).

5. Conclusions

The detection of HCN in high excitation states clearly demonstrates that it is formed in the inner part of the envelope of χ Cyg, within $\gtrsim 20R_\star$. This is strongly supported by detailed chemical modelling of the atmosphere. The earlier claim of HCN along with other carbon bearing molecules being formed in the inner-most region of the envelope of O -rich star like IK Tau (DCW99) seems to be true in the case of S type star χ Cyg as well. This is the first observational verification of the theoretical claim that shock chemistry plays an active role in defining the chemical composition of the inner wind regions of Miras.

References

Bedding T. R., Zijlstra A., 1998, ApJ 506, L47
Bieging J. H., Latter W. B., 1994, ApJ 442, 765 (BL94)
Bertschinger E., Chevalier R. A., 1985, ApJ 299, 167
Bujarrabal V., Fuente A., Omont A., 1994, A&A 285, 247
Cherchneff I., Barker J. R., Tielens A. G. G. M., 1992, ApJ 401, 269
Duari D., Cherchneff I., Willacy K., 199, A&A 341, L47 (DCW99)
Fox M. W., Wood P. R., 1982, ApJ 259, 198
Goldsmith P. F., Snell R. L., Deguchi S., Krotkov R., Linke R. A. 1982, ApJ 260, 147
Haniff C. A., Scholz M., Tuthill P. G., 1995, MNRAS 276, 640
Lucas R., Guilloteau S., 1992, A&A 259, L23
Perryman M. A. C., Lindegren L., Kovalevsky J., Hog E., Bastian U., et al., 1997, A&A 323 L49
Sopka R. J., Olofsson H., Johansson L. E. B., Nguyen-Q-Rieu, Zuckerman B., 1989, A&A 210, 78
Stutzki J., Genzel R., Harris A. I., Herman J., 1988, ApJ 330, L125
Tuthill P. G., Haniff C. A., Baldwin J. E., 1999, MNRAS 306, 353
Willacy K., Millar T. J., 1997, A&A 324, 237
Willacy K., Cherchneff I., 1998, A&A 330, 676
Ziurys L., Turner B., 1986, ApJ 300, L19